Mussel-Inspired Direct Immobilization of Nanoparticles and Application for Oil–Water Separation

Qing Zhu and Qinmin Pan*

School of Chemical Engineering and Technology, Harbin Institute of Technology, Harbin 150001, P. R. China

ABSTRACT Immobilization of various nanoparticles onto complex 2D or 3D macroscopic surface is an important issue for nanotechnology, but the challenge remains to explore a facile, general and environmentally friendly method for achieving this goal. Taking inspiration from the adhesion of marine mussels, we reported here that oxide nanoparticles of different compositions and sizes were directly and robustly anchored on the surface of monolithic foams ranging from polymer to metals in an aqueous solution of dopamine. The effective immobilization of the nanoparticles was strongly dependent on the oxidation of dopamine, which could be tuned by either pH or by adding *n*-dodecanethiol. Interestingly, the thiol addition not only allowed the immobilization to take place in a wide pH range, but also led to superhydrophobicity of the resulting foams. Application of the superhydrophobic foams was illustrated by fast and selective collecting oils from water surface. Because catecholic derivatives exhibit high affinity to a variety of substances, the present strategy might be extendable to fabricate hybrid nanomaterials desirable for self-cleaning, environmental protection, sensors and catalysts, and so forth.

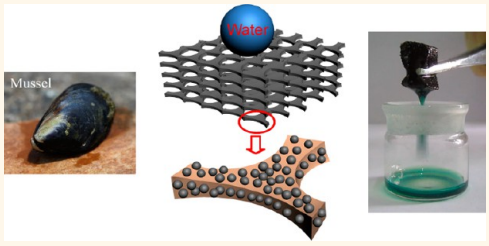

KEYWORDS: mussel-inspired · oxide nanoparticles · immobilization · porous substrates · superhydrophobicity · oil–water separation

Immobilization of nanoparticles (NPs) onto complex two- (2D) and three-dimensional (3D) structures has a wide spectrum of applications in optics and electronics,[1,2] biomedicine,[3,4] sensors,[5,6] energy storage,[7] catalysis,[8] and so on.[9,10] A number of strategies have been proposed for achieving this goal, which mainly involved the modification of either nanoparticles or target surfaces with polymers,[11] supramolecular assemblies[12] and molecules containing functional groups such as mercapto,[13] pyridyl,[14] amino,[15], diazonium salt,[16] *etc.* The immobilization mechanism mainly depends on noncovalent interactions[17–19] or covalent bonding[20,21] between nanoparticles and surfaces. However, most of the existing methods are either complicated in operations or only suitable for one class of 2D surfaces and nanoparticles. The challenge remains to develop a facile strategy capable of directly anchoring various nanoparticles onto different macroscopic 3D substrates under mild conditions, without considering their nature and morphologies. In addition, exploring novel properties and potential applications of the immobilized nanoparticles is also important for nanotechnology.

In nature, marine mussels adhere to virtually all types of substrates with high binding strength under wet conditions by secreting *Mytilus edulis* foot protein (mfp-3).[22,23] Recent studies revealed that high levels of catecholic analogues (3,4-dihydroxy-phenylalanine, DOPA) presented in mfp-3 mainly account for the strong adhesion of mussels.[24,25] Although the mechanism for the catecholic adhesion is rather complicated, it is believed to originate from covalent binding as well as noncovalent interfacial interactions between substrates and catecholic derivatives of either small molecules or macromolecules.[26–28] In this regard, the adhesion of mussel protein might offer us an alternative strategy for immobilizing nanoparticles on solid surfaces under mild wet conditions.

Herein, inspired by the bioadhesion of marine mussels, we reported that nanoparticles of different sizes and chemical compositions were anchored separately or together onto macroscopic porous substrates ranging from polymer to metals in an aqueous solution of dopamine, without

* Address correspondence to panqm@hit.edu.cn.

Received for review October 7, 2013 and accepted January 9, 2014.

Published online January 09, 2014
10.1021/nn4052277

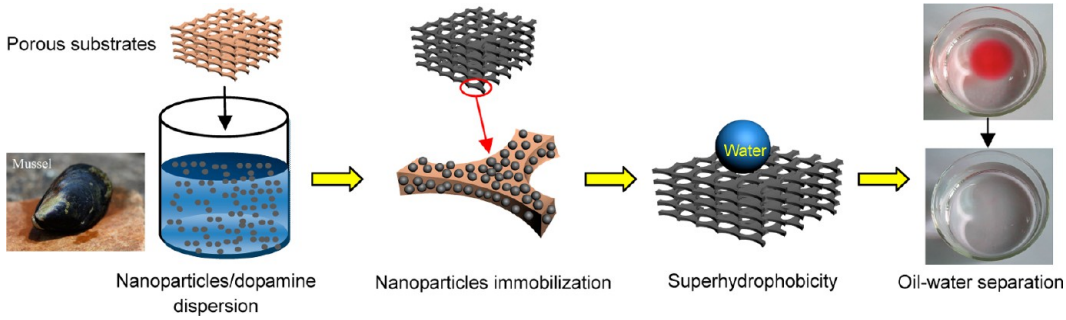

Scheme 1. Illustration for the immobilization of nanoparticles onto porous substrates and application for oil−water separation.

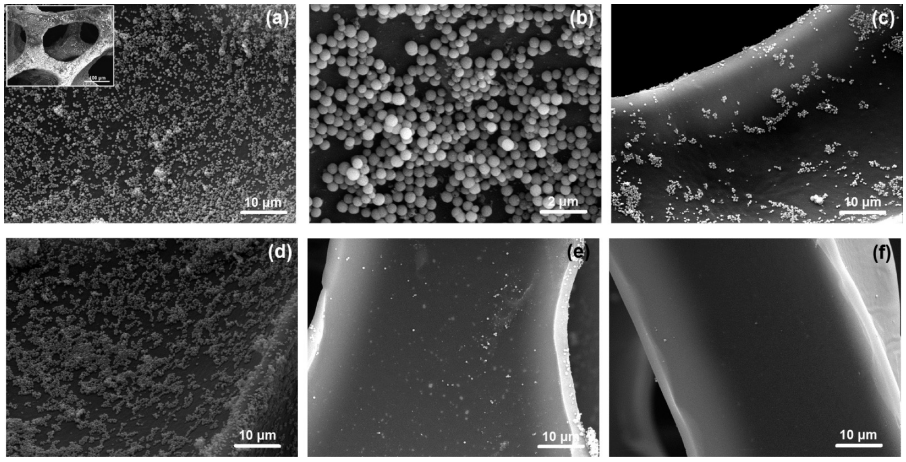

Figure 1. SEM images of the sponges treated in aqueous dopamine/Fe_3O_4 dispersions at pH 1 (a and b), pH 3 (d), pH 5 (e), and pH 7 (f); (c) is the SEM image of a sponge treated in aqueous Fe_3O_4 dispersion without dopamine at pH 1.

specific functionalization of either substrates or nanoparticles. More interesting was that adding *n*-dodecanethiol to the solution not only allowed the immobilization to take place in a wide pH range, but also led to superhydrophobicity of the resulting substrates. Superhydrophobic polyurethane (PU) sponges fabricated by this strategy exhibited high selectivity and recyclability for oil−water separation (Scheme 1). Although numerous reports mimicked the strong adhesion of mussels by using catechol-containing polymers over the past few years,[26−30] to our knowledge, rare studies focused on small catecholic derivatives with an aim for directly immobilizing nanoparticles and fabricating superhydrophobic surfaces. Therefore, these findings offer a facile and versatile strategy to fabricate hybrid nanomaterials desirable for potential applications such as sensors, self-cleaning, environmental protection, catalysts, and so on.

RESULTS AND DISCUSSION

To investigate the notion of direct nanoparticle-immobilization by dopamine, we used Fe_3O_4 nanoparticles (Figure S1a, Supporting Information) and commercial polyurethane (PU) sponge as target substances. In a typical experiment, Fe_3O_4 nanoparticles and a piece of PU sponge were added to an aqueous solution of dopamine (10.5 mmol L^{-1}) and the resulting mixture was stirred for 12 h. Here we controlled the pH of the solution at 1 to retard the oxidation of dopamine.[31] Figure 1a,b displays the SEM images of the resulting sponge. They show that Fe_3O_4 nanoparticles of ~450 nm densely and homogenously cover the outer and inner surface of the sponge. In contrast, only very low amount of Fe_3O_4 nanoparticles coats the sponge treated in Fe_3O_4 dispersion without dopamine at the same pH (Figure 1c), indicating the important role of dopamine in the nanoparticle adhesion process. The results imply that dopamine can directly "glue" Fe_3O_4 nanoparticles to the sponge skeleton, while avoiding specific modification of nanoparticles and substrates of the previous reports.[4−21]

The immobilization process strongly depended on the acidity of aqueous dopamine/Fe_3O_4 dispersions. A sponge treated in the dispersion at pH 3 also displayed densely anchored nanoparticles, but its coverage was lower than that treated at pH 1 (Figure 1d). However, Fe_3O_4 coverage decreased significantly as the pH of the dispersions was higher than 3 (Figure 1e,f). In fact, almost no Fe_3O_4 nanoparticles covered the sponges even under moderately acidic conditions (*e.g.*, pH 5). The decrease in Fe_3O_4 coverage indicates a pH-induced chemical or structural change in dopamine.

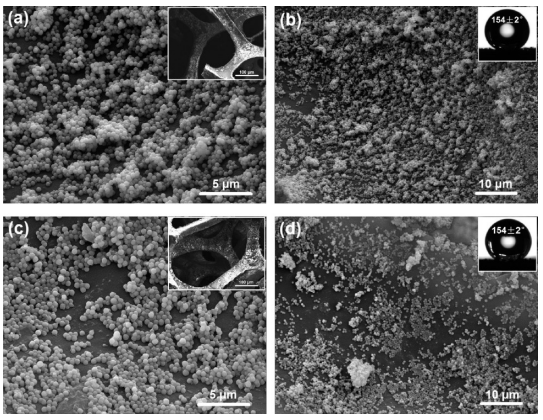

Figure 2. SEM images and water contact angles of the sponges treated in aqueous dopamine/Fe_3O_4 dispersions containing *n*-dodecanethiol at pH 7 (a and b) and pH 11 (c and d).

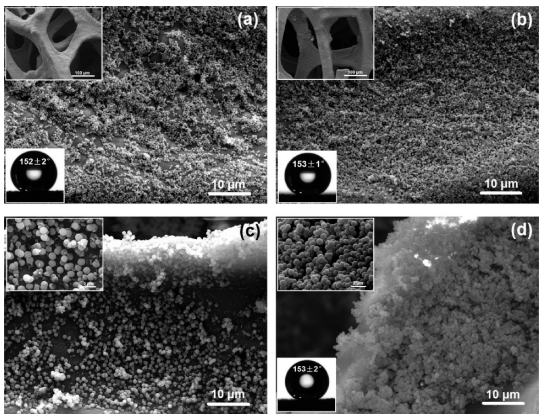

Figure 3. SEM images and water contact angles of the nickel foam (a) and copper foam (b) treated in aqueous dopamine/Fe_3O_4 dispersions containing *n*-dodecanethiol at pH 7. (c and d) SEM images of the sponges treated in the (c) aqueous dopamine/SiO_2 dispersion at pH 1 and (d) aqueous dopamine/SiO_2 dispersion containing *n*-dodecanethiol at pH 7.

Most likely the change might be associated with the oxidation of dopamine into *o*-quinone at elevated pH.[31−33] Indeed, ultraviolet−visible (UV−vis) spectra and optical images revealed that dopamine was stable for hours at pH 5 in solution and spontaneously oxidized at pH 7 (Figure S2, Supporting Information). The above-mentioned results suggest that the oxidation of dopamine into *o*-quinone greatly reduces the adhesion between Fe_3O_4 nanoparticles and the sponges, leading to the failure of the immobilization process.

Since the oxidation of dopamine is mainly responsible for the ineffective immobilization of Fe_3O_4 nanoparticles, it is reasonable that adding antioxidant to dopamine solution might contribute to the immobilization process taking place at a higher pH. In nature, mussels retard the oxidation of DOPA by co-secreting thiol-rich proteins (mfp-6) as antioxidants during plaque deposition.[34,35] To investigate this possibility, we added *n*-dodecanethiol (2.1 mmol L^{-1}) to the dopamine/Fe_3O_4 dispersion at pH 7. SEM images of the resulting sponge clearly show a dense and homogeneous coverage of Fe_3O_4 nanoparticles (Figure 2a,b). Interestingly, Fe_3O_4 nanoparticles also anchored on the surface of sponge even under strong alkaline conditions of pH 11 (Figure 2c,d). These images are in contrast with those of the counterparts treated in the same dispersion without *n*-dodecanethiol (Figure 1f, Figure S3 of Supporting Information). The reason for the effective immobilization at high pH is that *n*-dodecanethiol retards the oxidation of dopamine to some extent (Figure S4, Supporting Information) and the adhesion of dopamine is kept even in alkaline conditions. Although the effect of thiol structure on the immobilization of nanoparticles deserves further investigation, *n*-dodecanethiol addition enables the process to occur in a wide pH range from 1 to 11.

More interesting, the surface of the resulting sponge exhibited superhydrophobicity (*i.e.*, lotus effect) and water contact angles of 154 ± 2° (Figure 2b,d). It also showed a hysteretic angle of 7 ± 2°. The surface composition of the superhydrophobic sponge was characterized by XPS analysis, which showed the presence of chemically bound thiolate species (Figure S5, Supporting Information). The bound thiolate species indicate the grafting of *n*-dodecanethiol molecules to *o*-quinone through Michael addition (Figure S6, Supporting Information).[36] Generally, the superhydrophobicity of a solid surface is dependent on hierarchical roughness as well as low surface energy.[37,38] In this case, homogeneously anchored nanoparticles enhance the surface roughness, while the grafted *n*-dodecanethiol reduces the surface energy of the sponge. Recently, Xu *et al.*[39] reported a family of superhydrophobic particles by using polydopamine as interlayer. However, this method involved subsequent deposition of silver nanoparticles and thiol modification. Moreover, it was only reported for particulate substrates. In contrast, the present approach directly fabricated superhydrophobic surfaces by immobilizing both nanoparticles and *n*-dodecanethiol molecules onto monolithic porous substrates, while avoiding multiple operation processes and complicated instruments. Therefore, the thiol addition not only extends the immobilization process in a wide pH range, but also provides a one-step and mild method for fabricating superhydrophobic surfaces that have potential applications for self-cleaning and oil−water separation, and so on.

The versatility of the present strategy was demonstrated by using different types of porous substrates and nanoparticles. Fe_3O_4 nanoparticles were effectively immobilized on other porous substrates like nickel foam and copper foam at pH 1−11 (Figure 3a,b, Figures S7 and S8 of Supporting Information), and the resulting foams showed superhydrophobic properties. Compared with PU sponges, the metallic counterparts

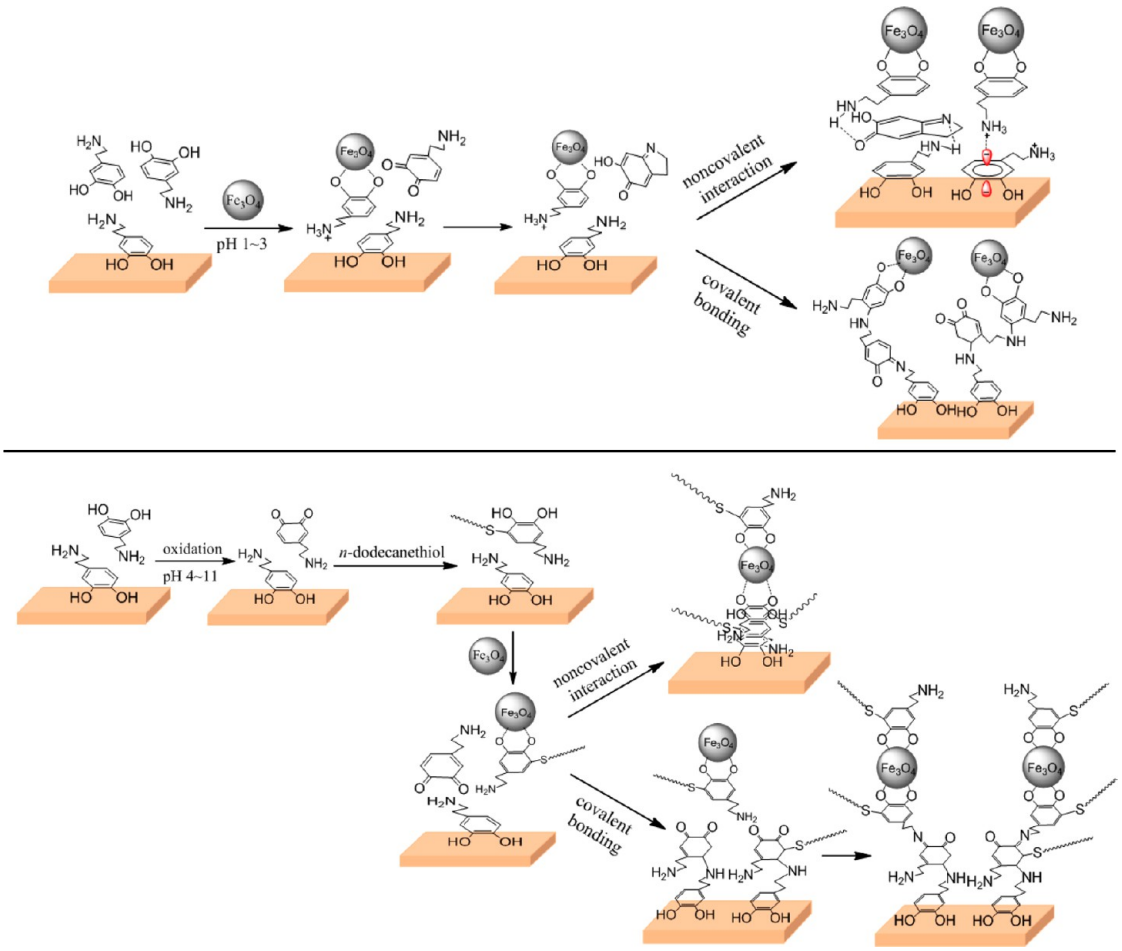

Scheme 2. Proposed mechanism for the immobilization of Fe_3O_4 nanoparticles and *n*-dodecanethiol molecules.

exhibited a more homogeneous and denser coverage of the nanoparticles. This difference is believed to arise from the coordination between dopamine with the metallic substrates,[26,28] leading to a higher immobilization efficiency. Furthermore, we used SiO_2 nanoparticles of ~900 nm (Figure S1b, Supporting Information) to perform the similar experiment on PU sponge. SiO_2 nanoparticles were evenly anchored on the sponge skeleton with a high coverage (Figure 3c,d). Interestingly, a mixture of nanoparticles with different sizes and chemical compositions could be directly immobilized onto sponges, allowing us to combine multifunctions from different nanoparticles in a single procedure. For instance, silica and Fe_3O_4 nanoparticles were simultaneously anchored onto the surface of sponge skeletons (Figure S9, Supporting Information). As a result, the mussel-inspired strategy is applicable to porous substrates varying from low surface-energy polymers to high surface-energy metals, as well as oxides nanoparticles with different natures and sizes.

The robustness of the immobilized Fe_3O_4 nanoparticles was tested by ultrasonication in ethanol for 5, 10, 15, and 20 min. SEM observations showed that Fe_3O_4 nanoparticles anchored on the sponge were able to withstand sonication for 10 min without significant decrease in coverage. Nevertheless, considerable fraction of the nanoparticles was detached from the sponge after sonication for 20 min (Figure S10, Supporting Information). In comparison, Fe_3O_4 nanoparticles covered on the nickel foam were more robust than those on the sponge, which might relate to the coordination between catecholic moiety and nickel[26,28] (Figure S11, Supporting Information).

On the basis of above results, we propose a possible mechanism for the immobilization of Fe_3O_4 nanoparticles and *n*-dodecanethiol molecules (Scheme 2). Under acidic conditions, considerable amounts of dopamine molecules anchor on Fe_3O_4 nanoparticles[40] and the substrates through bidentate modes of either H-bonding or metal coordination (depending on the nature of target substances), forming "anchoring sites" for the subsequent immobilization process (Figure S12, Supporting Information).[26,28,41] Although high acidity retards the oxidation of dopamine to some extent, trace amount of dopamine is still oxidized to *o*-quinone with high reactivity to amino and mercapto groups.[34−36,42] In this study, the resulting *o*-quinone plays an important role in the immobilization process by linking the dopamine anchored on the nanoparticles and substrates. On one hand, part of *o*-quinone might directly

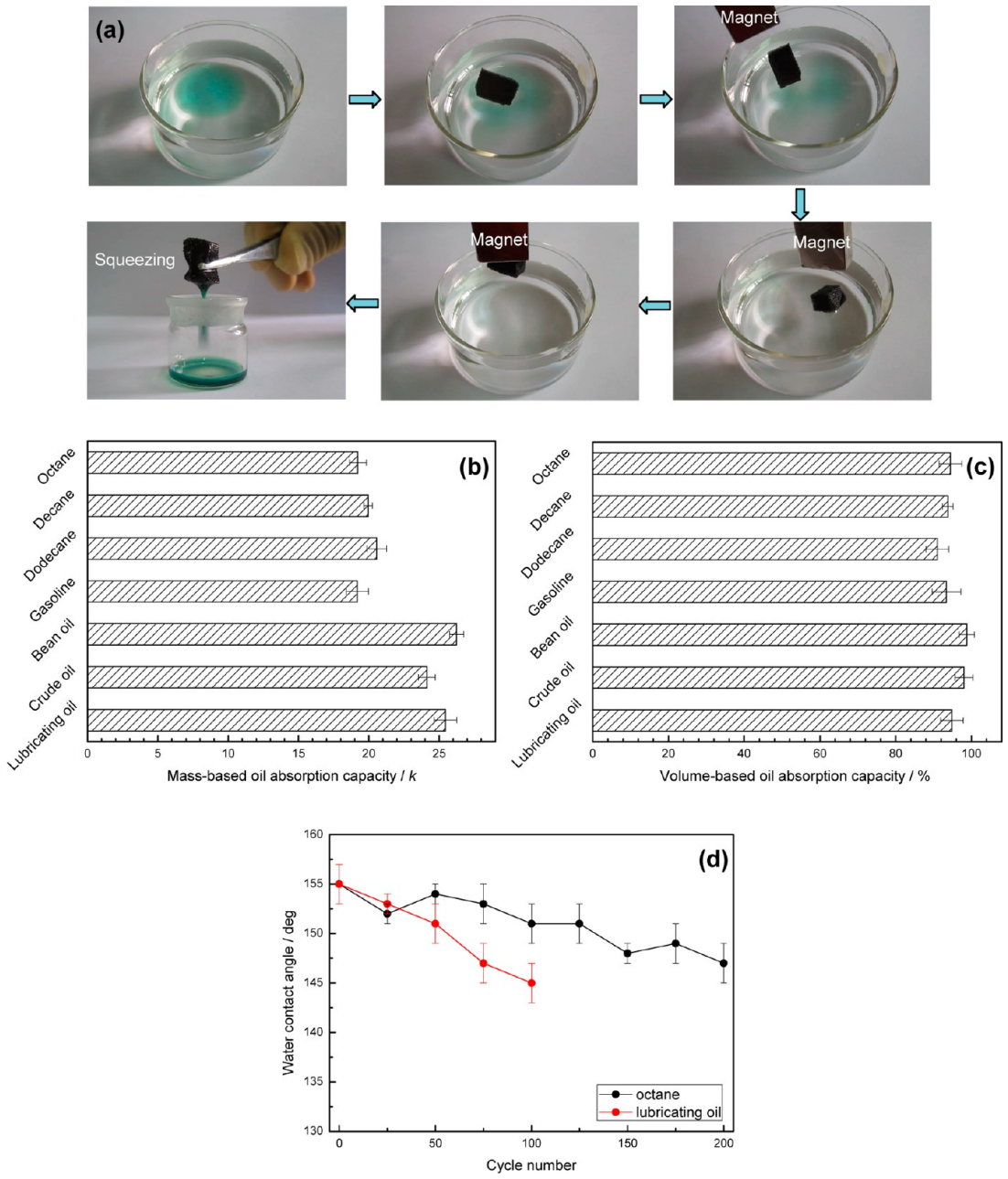

Figure 4. (a) Collection of lubricating oil from water surface by a superhydrophobic sponge under magnetic field; mass-based (b) and volume-based (c) oil-absorption capacities of the sponge; water contact angles (d) recorded for the sponge after each oil−water separation process.

react with $-NH_2$ group of the anchored dopamine *via* intermolecular Schiff base reaction and/or Michael addition (Figure S13, Supporting Information).[43] Another possibility is that *o*-quinone is converted to compounds like dopaminechrome, 5,6-dihydroxyindole (DHI) and so on *via* intramolecular Michael addition.[24,27,44] The resultant compounds form intermolecular interactions with the anchored dopamine through H-bonding, $\pi-\pi$ stacking, $\pi-$cation interaction, *etc* (Figure S13, Supporting Information).[26−28,44,45] Since forming sufficient "anchoring sites" on the nanoparticles and substrates is a prerequisite for the effective immobilization process, elaborately controlling the oxidation of dopamine (or relative content of *o*-quinone) is a crucial step. In alkaline conditions, a large amount of dopamine is oxidized to *o*-quinone, thus greatly reducing the content of dopamine anchored on the nanoparticles and substrates. The lack of anchored dopamine causes the failure of the nanoparticle-immobilization process. However, the oxidation of dopamine is greatly retarded by adding *n*-dodecanethiol because thiol is an effective reducing agent for *o*-quinone.[34−36] The thiol addition not only regenerates dopamine but also produces catecholic moieties grafted with thiolate species (Figure S6, Supporting Information),[34−36] which largely decreases the relative content of *o*-quinone.

These catecholic derivatives then anchor onto the nanoparticles and substrates to form "anchoring sites", while trace *o*-quinone links the "anchoring sites" through covalent bonding and noncovalent interactions, resulting in the immobilization of the nanoparticles. It is reasonable that the anchoring of thiolate-grafted catecholic moieties gives rise to superhydrophobicity of the substrates. Although detail mechanism for the immobilization is complicated and deserves further investigations, we believe that both covalent bonding and noncovalent interactions might account for the effective immobilization of the nanoparticles and thiol molecules on the substrates.

As an example for applications, a piece of superhydrophobic sponge fabricated in this study was used for separating oils from water. By simply placing the sponge on the surface of oil–water mixtures, we were able to quickly and selectively remove oils including lubricating oil, crude oil, and octane from the water in a few seconds. Owing to the presence of Fe_3O_4 nanoparticles, the sponge could be manipulated to the oil-polluted region by a magnet bar, providing a magnetic-actuated method for oil-removal. Interestingly, the absorbed oils were readily collected from the sponge through a simple mechanical squeezing process (Figure 4a). The mass-based absorption capacities for the oils are in the range of 18–26 (Figure 4b), which is comparable to those of other polymer-based counterparts.[46–49] However, the sponge shows very high volume-based absorption capacities greater than 90% (Figure 4c), indicating that almost all of its volume is used for oil-storage. Compared with other reported absorptive materials like nanocellulose aerogel, magnetic foam, graphene foams and carbon nanotube sponge,[46,49–52] the present sponge exhibits one of the highest space-utilizations for oil-storage. Importantly, the superhydrophobic sponge could be reused for oil–water separation for many cycles. Figure 4d records the water contact angles of the sponge after each separation process. The sponge still exhibits a water contact angle greater than 150° after separating octane for 125 cycles. Excellent recyclability of the sponge originates from the robustness of the immobilized nanoparticles, as evidenced by the SEM images in Figures S10 and S11. Nevertheless, the sponge lost superhydrophobicity after the separation of lubricating oil from water for 50 cycles. The decrease in recyclability is related to the high viscosity of lubricating oil, which results in the detachment of Fe_3O_4 nanoparticles from the sponge skeleton in the squeezing process. The above results provide a facile and efficient approach for cleaning oils from water surface.

CONCLUSIONS

Taking inspiration from mussel adhesion, we reported a one-step and versatile strategy for the robust immobilization of oxides nanoparticles and fabrication of superhydrophobic surfaces for the first time. The effective immobilization of the nanoparticles strongly depended on the oxidation of dopamine, which could be tuned by pH or adding *n*-dodecanethiol. Interestingly, the thiol addition made the immobilization take place in a wide pH range by retarding the oxidation of dopamine, as well as led to superhydrophobicity of the resulting foams. The superhydrophobic PU sponges obtained by the strategy effectively separated oils from water surface through a magnetic-actuated manner, and exhibited one of the highest space-utilizations for oil-storage among the reported counterparts. A possible mechanism for the immobilization of the nanoparticles and thiol molecules might be associated with the adhesive properties of dopamine as well as the high reactivity of *o*-quinone. Considering high adhesion of catecholic derivatives to almost all inorganic and organic substances, this approach might be extendable for various nanoparticles and different substrates, regardless of nature and morphology. With an elaborate choice of starting materials, multifunctional nanomaterials might be fabricated for self-cleaning, environmental remediation, catalysts, biosensors, and so on.

MATERIALS AND METHODS

Materials. Polyurethane (PU) sponges (88% in porosity and 200–250 μm in pore size) were provided by Qingdao Yuquan Sponge Product Co., Ltd. (China). Nickel and copper foams (80–83% in porosity and 160–400 μm in pore size) were purchased from Wuzhou Sanhe New Mater Co., Ltd. (Guangxi, China). Dopamine hydrochloride was supplied by BASF Chemicals, Tianjin Co., Ltd. (China). Iron(III) chloride hexahydrate ($FeCl_3 \cdot 6H_2O$), sodium acetate trihydrate ($NaAc \cdot 3H_2O$), sodium hydroxide (NaOH), tetraethoxysilane ($C_8H_{20}O_4Si$, TEOS), ammonia solution ($NH_3 \cdot H_2O$, 25 wt %), hydrochloric acid (HCl), ethylene glycol ($C_2H_6O_2$) and *n*-dodecanethiol (n-$C_{12}H_{25}SH$) were supplied by Tianjin Kermel Chemical Reagent Co., Ltd. (China).

Synthesis of Fe_3O_4 Nanoparticles. A total of 1.35 g of $FeCl_3 \cdot 6H_2O$ was dissolved in 40 mL of ethylene glycol, followed by addition of 3.6 g of sodium acetate (NaAc) with stirring for 30 min to form a homogeneous solution. Then the solution was sealed in an autoclave and heated at 200 °C for 15–18 h.[53] After the autoclave was cooled to room temperature, black powder was successively washed by ethanol and water five times to obtain Fe_3O_4 nanoparticles with ~450 nm in diameter.

Synthesis of SiO_2 Nanoparticles. Three milliliters of tetraethoxysilane (TEOS) and 10 mL of $NH_3 \cdot H_2O$ (25 wt %) were added to 50 mL of isopropyl alcohol, and the resulting mixture was vigorously stirred for 6 h. Then 3 mL of TEOS and 5 mL of $NH_3 \cdot H_2O$ were added again to the above mixture. After it stirred for another 12 h, the mixture was separated by centrifugation and the solid residue was washed by water five times.[54] SiO_2 nanoparticles with ~900 nm in diameter were obtained.

Immobilization of Nanoparticles to Porous Substrates. Before use, PU sponges (1 cm × 1 cm × 0.5 cm) were ultrasonically cleaned in water and ethanol for 10 min, respectively, while nickel and copper foams (1 cm × 1 cm × 0.2 cm) were washed in a diluted HCl solution for 1 min and then rinsed with water. In a typical

experiment, 100 mg of nanoparticles (Fe_3O_4, SiO_2, or the mixture of Fe_3O_4 and SiO_2) and 40 mg of dopamine hydrochloride were dispersed in 20 mL of H_2O at pH = 1, 3, 5, 7, 9, and 11 by ultrasonication. The pH of the dispersions was adjusted by hydrochloric acid or NaOH. Then a piece of PU sponge was immersed in the above dispersions under stirring for 12 h. After it was rinsed with water and dried at 80 °C, the sponge covered with nanoparticles was obtained. The above process was also performed on nickel and copper foams in dopamine/nanoparticles dispersions at pH 1−3.

Fabrication of Superhydrophobic Foams. A total of 100 mg of nanoparticles (Fe_3O_4, SiO_2, or the mixture of Fe_3O_4 and SiO_2), 40 mg of dopamine hydrochloride and 10 μL of *n*-dodecanethiol were dispersed in 20 mL of H_2O/ethanol solution (1:1 v/v) at pH 4−11 by ultrasonication. Then a piece of PU sponge (nickel or copper foams) was immersed in the resulting dispersions under stirring for 12 h. After it was rinsed with water and dried at 80 °C, superhydrophobic sponge (nickel or copper foams) was obtained.

Control Experiments. A total of 100 mg of Fe_3O_4 nanoparticles was dispersed in 20 mL of H_2O at pH 1 without dopamine hydrochloride by ultrasonication. Then a piece of PU sponge was immersed in the dispersion under stirring for 12 h. The resulting sponge was rinsed with water and dried at 80 °C.

Collection of Oils from Water Surface. Seven kinds of oils including octane, *n*-decane, *n*-dodecane, gasoline, bean oil, crude oil, and lubricating oil were used in this study. A piece of superhydrophobic PU sponge was placed on oil−water mixtures (oils were dyed blue for clear observation). The sponge was driven to the oil-polluted region and then removed from the water surface by a magnet. The absorbed oils were collected through a simple squeezing process by tweezers. After each separation process, the sponge was washed with acetone and dried, and its water contact angle (CA) was measured. Oil-absorption capacities were calculated by weight or volume measurements according to previous reports.[46,50]

Characterizations. Morphology observations and energy dispersive X-ray (EDX) analysis of the samples were conducted on a scanning electron microscope (SEM, FEI Quanta 200). X-ray diffraction (XRD) patterns were recorded by a Shimadzu XRD-6000. X-ray photoelectron spectroscopy (XPS) was performed on a PHI-5700ESCA. Water contact angles (CAs) and hysteretic angles were measured by an OCA 20 (DataPhysics Instruments) with 3 μL water droplets as indicators. Ultraviolet−visible (UV−vis) spectra were recorded by a SPU-1900 spectrophotometer (Shanghai Spectrum Instruments, China). Liquid chromatography−mass spectrometry (LC−MS) was performed on an Accurate-Mass Q-TOFLC/MS (Agilent Technologies 6520).

Conflict of Interest: The authors declare no competing financial interest.

Acknowledgment. This work was financially supported by a self-planned task of the State Key Laboratory of Robotics and System of Harbin Institute of Technology (SKLRS200901C). The authors thank Prof. Yinyong Sun for gas chromatography−mass spectrometry measurements and consistent support.

Supporting Information Available: XRD patterns of Fe_3O_4 and SiO_2 nanoparticles, optical images and UV−vis spectra of aqueous dopamine solutions, XPS spectra of superhydrophobic sponges and dopamine-anchored Fe_3O_4 nanoparticles, SEM images of PU sponges, nickel foams and copper foams treated in different aqueous dopamine/Fe_3O_4 dispersions and MS results. This material is available free of charge *via* the Internet at http://pubs.acs.org.

REFERENCES AND NOTES

1. Klein, D. L.; Roth, R.; Lim, A. K. L.; Alivisatos, A. P.; McEuen, P. L. A Single-Electron Transistor Made from a Cadmium Selenide Nanocrystal. *Nature* **1997**, *389*, 699–701.
2. Shipway, A. N.; Katz, E.; Willner, I. Nanoparticle Arrays on Surfaces for Electronic, Optical and Sensor Applications. *ChemPhysChem* **2000**, *1*, 18–52.
3. Michalet, X.; Pinaud, F. F.; Bentolila, L. A.; Tsay, J. M.; Doose, S.; Li, J. J.; Sundaresan, G.; Wu, A. M.; Gambhir, S. S.; Weiss, S. Quantum Dots for Live Cells, *in Vivo* Imaging, and Diagnostics. *Science* **2005**, *307*, 538–544.
4. Tang, D. P.; Yuan, R.; Chai, Y. Q. Direct Electrochemical Immunoassay Based on Immobilization of Protein-Magnetic Nanoparticle Composites on to Magnetic Electrode Surfaces by Sterically Enhanced Magnetic Field Force. *Biotechnol. Lett.* **2006**, *28*, 559–565.
5. Elghanian, R.; Storhoff, J. J.; Mucic, R. C.; Letsinger, R. L.; Mirkin, C. A. Selective Colorimetric Detection of Polynucleotides Based on the Distance-Dependent Optical Properties of Gold Nanoparticles. *Science* **1997**, *277*, 1078–1081.
6. Petryayeva, E.; Krull, U. J. Quantum Dot and Gold Nanoparticle Immobilization for Biosensing Applications Using Multidentate Imidazole Surface Ligands. *Langmuir* **2012**, *28*, 13943–13951.
7. Yang, S.; Li, G.; Zhu, Q.; Pan, Q. Covalent Binding of Si Nanoparticles to Graphene Sheets and Its Influence on Lithium Storage Properties of Si Negative Electrode. *J. Mater. Chem.* **2012**, *22*, 3420–3425.
8. Praharaj, S.; Nath, S.; Ghosh, S. K.; Kundu, S.; Pal, T. Immobilization and Recovery of Au Nanoparticles from Anion Exchange Resin: Resin-Bound Nanoparticle Matrix as a Catalyst for the Reduction of 4-Nitrophenol. *Langmuir* **2004**, *20*, 9889–9892.
9. Kiely, C. J.; Fink, J.; Brust, M.; Bethell, D.; Schiffrin, D. J. Spontaneous Ordering of Bimodal Ensembles of Nanoscopic Gold Clusters. *Nature* **1998**, *396*, 444–446.
10. Kameyama, T.; Ohno, Y.; Kurimoto, T.; Okazaki, K. I.; Uematsu, T.; Kuwabata, S.; Torimoto, T. Size Control and Immobilization of Gold Nanoparticles Stabilized in an Ionic Liquid on Glass Substrates for Plasmonic Applications. *Phys. Chem. Chem. Phys.* **2010**, *12*, 1804–1811.
11. Xu, H.; Hong, R.; Lu, T.; Uzun, O.; Rotello, V. M. Recognition-Directed Orthogonal Self-Assembly of Polymers and Nanoparticles on Patterned Surfaces. *J. Am. Chem. Soc.* **2006**, *128*, 3162–3163.
12. Crespo-Biel, O.; Dordi, B.; Reinhoudt, D. N.; Huskens, J. Supramolecular Layer-by-Layer Assembly: Alternating Adsorptions of Guest- and Host-Functionalized Molecules and Particles Using Multivalent Supramolecular Interactions. *J. Am. Chem. Soc.* **2005**, *127*, 7594–7600.
13. Mout, R.; Moyano, D. F.; Rana, S.; Rotello, V. M. Surface Functionalization of Nanoparticles for Nanomedicine. *Chem. Soc. Rev.* **2012**, *41*, 2539–2544.
14. Malynych, S.; Luzinov, I.; Chumanov, G. Poly(vinyl pyridine) as a Universal Surface Modifier for Immobilization of Nanoparticles. *J. Phys. Chem. B* **2002**, *106*, 1280–1285.
15. Sainsbury, T.; Ikuno, T.; Okawa, D.; Pacilé, D.; Fréchet, J. M. J.; Zettl, A. Self-Assembly of Gold Nanoparticles at the Surface of Amine- and Thiol-Functionalized Boron Nitride Nanotubes. *J. Phys. Chem. C* **2007**, *111*, 12992–12999.
16. Ktari, N.; Quinson, J.; Teste, B.; Siaugue, J. M.; Kanoufi, F.; Combellas, C. Immobilization of Magnetic Nanoparticles onto Conductive Surfaces Modified by Diazonium Chemistry. *Langmuir* **2012**, *28*, 12671–12680.
17. Zheng, Y.; Lalander, C. H.; Thai, T.; Dhuey, S.; Cabrini, S.; Bach, U. Gutenberg-Style Printing of Self-Assembled Nanoparticle Arrays: Electrostatic Nanoparticle Immobilization and DNA-Mediated Transfer. *Angew. Chem., Int. Ed.* **2011**, *50*, 4398–4402.
18. Brom, C. R. V. D.; Arfaoui, I.; Cren, T.; Hessen, B.; Palstra, T. T. M.; Hosson, J. T. M. D.; Rudolf, P. Selective Immobilization of Nanoparticles on Surfaces by Molecular Recognition Using Simple Multiple H-Bonding Functionalities. *Adv. Funct. Mater.* **2007**, *17*, 2045–2052.
19. Wanunu, M.; Popovitz-Biro, R.; Cohen, H.; Vaskevich, A.; Rubinstein, I. Coordination-Based Gold Nanoparticle Layers. *J. Am. Chem. Soc.* **2005**, *127*, 9207–9215.
20. Oh, S. K.; Kim, Y. G.; Ye, H.; Crooks, R. M. Synthesis, Characterization, and Surface Immobilization of Metal Nanoparticles Encapsulated within Bifunctionalized Dendrimers. *Langmuir* **2003**, *19*, 10420–10425.
21. Yamanoi, Y.; Yonezawa, T.; Shirahata, N.; Nishihara, H. Immobilization of Gold Nanoparticles onto Silicon

Surfaces by Si-C Covalent Bonds. *Langmuir* **2004**, *20*, 1054–1056.
22. Silverman, H. G.; Roberto, F. F. Understanding Marine Mussel Adhesion. *Mar. Biotechnol.* **2007**, *9*, 661–681.
23. Waite, J. H. Adhesion a La Moule. *Integr. Comp. Biol.* **2002**, *42*, 1172–1180.
24. Haeshin, L.; Dellatore, S. M.; Miller, W. M.; Messersmith, P. B. Mussel-Inspired Surface Chemistry for Multifunctional Coatings. *Science* **2007**, *318*, 426–430.
25. Lee, H.; Scherer, N. F.; Messersmith, P. B. Single-Molecule Mechanics of Mussel Adhesion. *Proc. Natl. Acad. Sci. U. S. A.* **2006**, *103*, 12999–13003.
26. Ye, Q.; Zhou, F.; Liu, W. Bio-Inspired Catecholic Chemistry for Surface Modification. *Chem. Soc. Rev.* **2011**, *40*, 4244–4258.
27. Hong, S.; Na, Y. S.; Choi, S.; Song, I. T.; Kim, W. Y.; Lee, H. Non-Covalent Self-Assembly and Covalent Polymerization Co-Contribute to Polydopamine Formation. *Adv. Funct. Mater.* **2012**, *22*, 4711–4717.
28. Josep, S.; Javier, S. P.; Felix, B.; Daniel, R. M. Catechol-Based Biomimetic Functional Materials. *Adv. Mater.* **2013**, *25*, 653–701.
29. Losic, D.; Yu, Y.; Aw, M. S.; Simovic, S.; Thierry, B.; Jonas, A. M. Surface Functionalisation of Diatoms with Dopamine Modified Iron-Oxide Nanoparticles: Toward Magnetically Guided Drug Microcarriers with Biologically Derived Morphologies. *Chem. Commun.* **2010**, *46*, 6323–6325.
30. Heo, J.; Kang, T.; Jang, S. G.; Hwang, D. S.; Spruell, J. M.; Killops, K. L.; Waite, J. H.; Hawker, C. J. Improved Performance of Protected Catecholic Polysiloxanes for Bioinspired Wet Adhesion to Surface Oxides. *J. Am. Chem. Soc.* **2012**, *134*, 20139–20145.
31. Anderson, T. J.; Yu, J.; Estrada, A. Y.; Waite, J. H.; Israelachvili, J. N. The Contribution of DOPA to Substrate-Peptide Adhesion and Internal Cohesion of Mussel-Inspired Synthetic Peptide Films. *Adv. Funct. Mater.* **2010**, *20*, 4196–4205.
32. Yu, J.; Wei, W.; Danner, E.; Israelachvili, J. N.; Waite, J. H. Effects of Interfacial Redox in Mussel Adhesive Protein Films on Mica. *Adv. Mater.* **2011**, *23*, 2362–2366.
33. Proudfoot, G. M.; Ritchie, I. M. A Cyclic Voltammetric Study of Some 4-Substituted Benzene-1,2 Diols. *Aust. J. Chem.* **1983**, *36*, 885–894.
34. Zhao, H.; Waite, J. H. Linking Adhesive and Structural Proteins in the Attachment Plaque of Mytilus Californianus. *J. Biol. Chem.* **2006**, *281*, 26150.
35. Yu, J.; Wei, W.; Danner, E.; Ashley, R. K.; Israelachvili, J. N.; Waite, J. H. Mussel Protein Adhesion Depends on Interprotein Thiol-Mediated Redox Modulation. *Nat. Chem. Biol.* **2011**, *7*, 588–590.
36. Wu, J.; Zhang, L.; Wang, Y.; Long, Y.; Gao, H.; Zhang, X.; Zhao, N.; Cai, Y.; Xu, J. Mussel-Inspired Chemistry for Robust and Surface-Modifiable Multilayer Films. *Langmuir* **2011**, *27*, 13684–13691.
37. Yao, X.; Song, Y. L.; Jiang, L. Applications of Bio-Inspired Special Wettable Surfaces. *Adv. Mater.* **2011**, *23*, 719–734.
38. Ganesh, V. A.; Raut, H. K.; Nair, A. S.; Ramakrishna, S. A. Review on Self-Cleaning Coatings. *J. Mater. Chem.* **2011**, *21*, 16304–16322.
39. Zhang, L.; Wu, J.; Wang, Y.; Long, Y.; Zhao, N.; Xu, J. Combination of Bioinspiration: A General Route to Superhydrophobic Particles. *J. Am. Chem. Soc.* **2012**, *134*, 9879–9881.
40. Xu, C.; Xu, K.; Gu, H.; Zheng, R.; Liu, H.; Zhang, X.; Guo, Z.; Xu, B. Dopamine as a Robust Anchor to Immobilize Functional Molecules on the Iron Oxide Shell of Magnetic Nanoparticles. *J. Am. Chem. Soc.* **2004**, *126*, 9938–9939.
41. Yu, J.; Wei, W.; Menyo, M. S.; Masic, A.; Waite, J. H.; Israelachvili, J. N. Adhesion of Mussel Foot Protein-3 to TiO_2 Surfaces: the Effect of pH. *Biomacromolecules* **2013**, *14*, 1072–1077.
42. Yu, M.; Hwang, J.; Deming, T. J. Role of L-3,4-Dihydroxyphenylalanine in Mussel Adhesive Proteins. *J. Am. Chem. Soc.* **1999**, *121*, 5825–5826.
43. Javier, S. P.; Josep, S.; Beatriz, G.; Cristina, B.; Teo, P.; Ramon, A.; Jordi, H.; Felix, B.; Daniel, R. M. Versatile Nanostructured Materials *via* Direct Reaction of Functionalized Catechols. *Adv. Mater.* **2013**, *25*, 2066–2070.
44. Daniel, R. D.; Daniel, J. M.; Benny, D. F.; Donald, R. P.; Christopher, W. B. Elucidating the Structure of Poly-(dopamine). *Langmuir* **2012**, *28*, 6428–6435.
45. Lu, Q.; Oh, D. X.; Lee, Y.; Jho, Y.; Hwang, D. S.; Zeng, H. Nanomechanics of Cation$-\pi$ Interactions in Aqueous Solution. *Angew. Chem., Int. Ed.* **2013**, *52*, 3944–3948.
46. Korhonen, J. T.; Kettunen, M.; Ras, R. H. A.; Ikkala, O. Hydrophobic Nanocellulose Aerogels as Floating, Sustainable, Reusable, and Recyclable Oil Absorbents. *ACS Appl. Mater. Interfaces* **2011**, *3*, 1813–1816.
47. Calcagnile, P.; Fragouli, D.; Bayer, I. S.; Anyfantis, G. C.; Martiradonna, L.; Cozzoli, P. D.; Cingolani, R.; Athanassiou, A. Magnetically Driven Floating Foams for the Removal of Oil Contaminants from Water. *ACS Nano* **2012**, *6*, 5413–5419.
48. Hayase, G.; Kanamori, K.; Fukuchi, M.; Kaji, H.; Nakanishi, K. Facile Synthesis of Marshmallow-Like Macroporous Gels Usable under Harsh Conditions for the Separation of Oil and Water. *Angew. Chem., Int. Ed.* **2013**, *52*, 1–5.
49. Zhu, Q.; Chu, Y.; Wang, Z.; Chen, N.; Lin, L.; Liu, F.; Pan, Q. Robust Superhydrophobic Polyurethane Sponge as Highly Reusable Oil-Absorption Material. *J. Mater. Chem. A* **2013**, *1*, 5386–5393.
50. Chen, N.; Pan, Q. Versatile Fabrication of Ultralight Magnetic Foams and Application for Oil-Water Separation. *ACS Nano* **2013**, *7*, 6875–6883.
51. Sun, H.; Xu, Z.; Gao, C. Multifunctional, Ultra-Flyweight, Synergistically Assembled Carbon Aerogels. *Adv. Mater.* **2013**, *25*, 2554–2560.
52. Gui, X.; We, J.; Wang, K.; Cao, A.; Zhu, H.; Jia, Y.; Shu, Q.; Wu, D. Carbon Nanotube Sponges. *Adv. Mater.* **2010**, *22*, 617–621.
53. Deng, H.; Li, X. L.; Peng, Q.; Wang, X.; Chen, J. P.; Li, Y. D. Monodisperse Magnetic Single-Crystal Ferrite Microspheres. *Angew. Chem., Int. Ed.* **2005**, *44*, 2782–2785.
54. Chen, S. L.; Dong, P.; Yang, G. H.; Yang, J. J. Characteristic Aspects of Formation of New Particles during the Growth of Monosize Silica Seeds. *J. Colloid Interface Sci.* **1996**, *180*, 237–241.